

# Next Generation JPL Ultra-Stable Trapped Ion Atomic Clocks

Eric Burt, Blake Tucker, Kameron Larsen, Robert Hamell, and Robert Tjoelker

Jet Propulsion Laboratory, California Institute of Technology, Pasadena, CA

Email: [eric.a.burt@jpl.nasa.gov](mailto:eric.a.burt@jpl.nasa.gov)

## Abstract

Over the past decade, trapped ion atomic clock development at the Jet Propulsion Laboratory (JPL) has focused on two directions: 1) new atomic clock technology for space flight applications that require strict adherence to size, weight, and power requirements, and 2) ultra-stable atomic clocks, usually for terrestrial applications emphasizing ultimate performance. In this paper we present a new ultra-stable trapped ion clock designed, built, and tested in the second category. The first new standard, L10, will be delivered to the Naval Research Laboratory for use in characterizing DoD space clocks.

## Introduction

For its atomic clock characterization activities, the Naval Research Laboratory (NRL) requires reference clocks with better stability than those being characterized. Traditionally this has been accomplished using hydrogen maser atomic clocks, but recently the stability of the clocks being characterized has approached or even exceeded that of the masers. Thus it is necessary to use a reference clock with better stability, particularly on long time scales, than a hydrogen maser. An analogous situation exists in JPL's Frequency Standards Test Lab (FSTL). This facility is charged with characterizing hydrogen masers that will be used in the NASA Deep Space Network and so a reference clock with better long-term stability than a maser is needed in the FSTL as well.

While there are notable exceptions, typical masers drift at the  $5 \times 10^{-16}$  to  $2 \times 10^{-15}/\text{d}$  level [1]. In 2002 the first operational multi-pole trapped ion clock (referred to as LITS-8) was installed at the USNO and demonstrated a drift rate of about  $1 \times 10^{-16}/\text{d}$  [2]. The multi-pole trap greatly reduces sensitivity to frequency shifts caused by variations in ion number, but the small observed drift rate of LITS-8 was later attributed to a residual number-dependent effect [3].

In 1996, JPL developed an implementable, continuously operating mercury ion clock based on a quadrupole ion trap for operation in the DSN (LITS 4-7)[4]. The standard could discipline several Local Oscillators, and could operate with a practical VCO as the Local Oscillator. In 1999, JPL introduced a specialized “multipole” trap design that greatly reduced systematic relativistic effects [5] and in 2002 JPL developed

implementable, continuously operating multipole based mercury ion clocks LITS-8 and LITS-9 [2]. (LITS-8 and 9 were still the size of a full rack).

In 2007-2008 JPL demonstrated exceptional long-term stability in a trapped ion clock that used a multi-pole ion trap coupled with a second-order Zeeman compensation scheme added to LITS-9 that virtually eliminated relativistic frequency shifts due to variations in the number of ions trapped [6]. Over a 9-month period of continuous unattended operation LITS-9 exhibited a drift of less than  $3 \times 10^{-17}$ /day relative to TT(BIPM07) [3, 7], the world ensemble of primary standards, making it significantly more stable than most hydrogen masers [1].

Based on the LITS-9 stability results and lessons learned from that unit, since 2010 we have been developing the next generation mercury trapped ion frequency standard (referred to as LITS-10 or L10). The immediate goal of L10 is to provide an advanced reference clock capability at the NRL and the JPL frequency standard test laboratories.

### Design goals of L10 – Lessons Learned from LITS-9

Much was learned from LITS-9 in achieving a high level of performance in a room temperature trapped ion clock. Table 1 shows the results of a stability evaluation of LITS-9 performed after the long run in 2007 [8].

TABLE I. SUMMARY OF LITS9 INSTABILITIES.

Effect	$\Delta f/f$ ( $\times 10^{-17}/\text{day}$ )	Uncertainty ( $\times 10^{-17}/\text{day}$ )
Second-order Doppler shift: ion temperature (neon pressure dependent)	-1.9	3.4
Pressure shift: neon	-1.4	0.6
Pressure shift: other background gas (assume: CH <sub>4</sub> worst case)	--	0.94
Second-order Doppler shift: ion number	-0.84	0.23
Second-order Zeeman shift: filament voltage	-0.35	0.14
Pressure Shift: neutral Hg	-0.22	0.40
Second-order Zeeman shift: external field	--	0.14
Second-order Zeeman shift: current source aging	-0.21	0.13
AC Zeeman shift: trap potential aging	< 0.00001	< 0.00001
AC Stark Shift: Black Body	-0.0001	0.00004
AC Stark Shift: Light Shift	+0.0001	0.0001
AC Stark Shift: Trapping Fields	< -0.00002	0.00002
Electronics Temperature Sensitivity	+0.11	+0.01 -0.09

The second-order Doppler shift due to variations in trapped ion number, previously the dominant systematic in this type of clock, had been reduced by the second-order Zeeman compensation to 4<sup>th</sup> on the list. The largest remaining systematic frequency perturbations were now due to variations in background gas pressure. To the extent these can be improved, LITS-9 stability performance can be improved even further.

To this end, changes were made to the L10 vacuum design including the capability for a much higher vacuum bakeout temperature and the flexibility to optimize performance with several different vacuum pump approaches. The compensation scheme used in LITS-9 was experimental so a goal for L10 was to engineer it into the design. The magnetic design for LITS-9 was a significant improvement over its predecessor units, offering improved shielding and better uniformity, however even further improvements were possible, particularly in conjunction with the inclusion of compensation into the design. Short-term stability in these clocks is dependent on the choice of the Local Oscillator (LO). Improvements in the signal-to-noise ratio (SNR) make it possible to consider new emerging LO technologies such as optical-to-microwave conversion [9]. Thus another L10 design goal was improvements in the input and output optical efficiencies, which determine the SNR. Finally, the design goals included replacing commercial electronics with custom DC-powered versions for lower power [10] and building the whole unit into a smaller, modular package with a path towards easier portability and industrialization.

## **L10 Design**

### *Built-in compensation*

Using the ion-number-dependent second order Zeeman shift to compensate the ion-number-dependent second order Doppler shift is accomplished by introducing a small magnetic inhomogeneity in the multi-pole trap region of the clock. In LITS-9 the magnetic inhomogeneity was introduced with a coil at one end of the C-field solenoid. Modeling showed that the primary effect was due to radial field inhomogeneity [6]. All solenoids have this and it can be made arbitrarily small by increasing the solenoid radius or decreasing the solenoid current.

In the case of LITS-9, the solenoid radius was small and the effect of changing ion number due to the magnetic field had the opposite sign (positive with increasing ion number) but a larger magnitude than that of the second order Doppler effect. Thus, the net ion-number-dependent shift was positive with increasing ion number.

In the design of L10, we wanted to “tune” the solenoid radius so that the magnetic effect was equal in magnitude but opposite that of the relativistic effect. However, the minimum field that this type of clock can reliably operate at to avoid decoherence due to coupling between Zeeman lines and motional side bands is about 60 mG. To operate at this field magnitude while compensating the number-dependent second order Doppler shift would require an unacceptably large solenoid radius. Instead, we make the L10

solenoid radius as large as possible within limits set by overall size constraints such that the demand on the additional compensation coil is minimized.

Figure 1 shows the change in frequency caused by varying the ion number by 36% with compensation off. The result of 1.1(2) mHz is a factor of 2x smaller than that for the same number change in LITS-9 (because the L10 solenoid has a larger radius), thereby realizing this design goal.

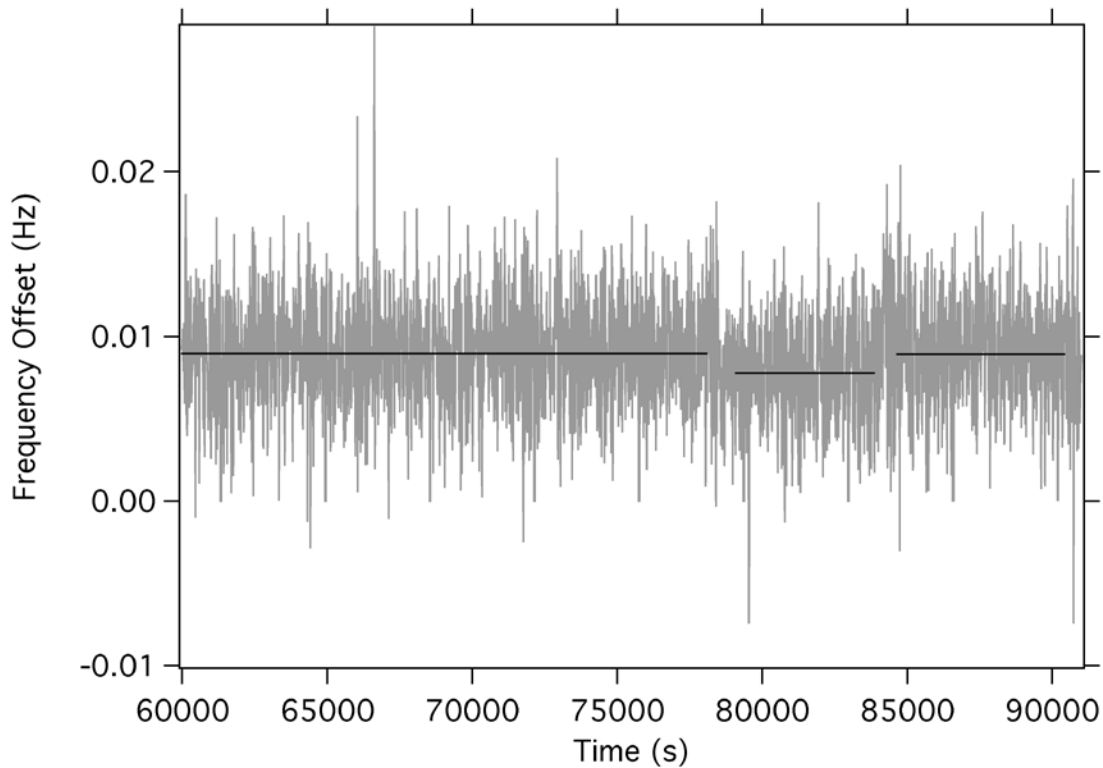


*Figure 1. Frequency offsets between L10 and a maser. For the middle segment, the ion number was reduced by 36% resulting in a frequency change of -1.1(2) mHz.*

*Sealed vacuum – reduce residual largest shifts: pressure stability*

As noted above, since the relativistic ion-number-dependent shift no longer dominates in a compensated multi-pole standard, the next largest effects are pressure-related.

Variations in background pressure have two broad sources: 1) variations in the neon buffer gas intentionally introduced for ion cooling purposes, and 2) outgassing: the evolution of gases from vacuum chamber walls.

In LITS-9, the vacuum chamber was operated with a turbo pump. Neon is readily pumped by the turbo and so a source is required. LITS-9 used a capillary leak, but even slow capillary leaks evolve as the source empties, leading to a small non-zero variation in clock frequency due to the neon/Hg<sup>+</sup> collision shift. In a sealed vacuum system with a

pump that has zero pumping speed for neon, a fixed amount of neon could be loaded, thereby eliminating fluctuations.

Due to limitations of certain vacuum components used in LITS-9, its vacuum bakeout temperature was limited to 200 C. A higher bakeout temperature would enable an exponentially lower outgassing rate and so lower frequency variations due to collision shifts with these gases, notably methane and hydrogen.

A fixed neon background is achieved in L10, as it has been in several ion clocks at JPL [11, 10], by using a sealed vacuum system with a getter pump. Getters only pump active gases and so do not pump neon, making them almost ideal for this application. One concern of the getter-pumped approach is other non-active gases not pumped by the getter, most notably methane. Other noble gases besides neon are not pumped, but have relatively small pressure shifts in Hg<sup>+</sup> and have no other deleterious effects. By contrast, methane is essentially non-reactive and has one of the largest known collision shift coefficients in Hg<sup>+</sup> [12]. Even a small change in methane concentration could significantly limit overall clock performance.

Initial experiments on a test system showed that methane increase in a high temperature baked getter-pumped system reaches acceptable levels after 1-2 months of equilibration time [8]. However the results of this measurement use an RGA to continually monitor methane pressure and it is known that the hot filament of the RGA (as well as an ion gauge) can crack methane into hydrogen and carbon, which are readily pumped by the getter [13].

As a further test, LITS-9 was converted to use only a getter. While it was still only bakeable to 200C, operation of LITS-9 with a getter could be used to place an upper bound on methane evolution and its impact on clock performance. Over a 1-year period of operation with a getter, LITS-9 demonstrated a drift rate of  $\sim 3 \times 10^{-17}$ /day, similar to its previous turbo-pumped performance, though the operation was not continuous. This puts an upper bound on methane evolution of also about  $1 \times 10^{-16}$  torr/s. It is important to note that this system also had an ion gauge present, which provided a hot filament to crack possibly evolving methane.

While the getter approach was promising, at this stage it was still not conclusive whether it would be useful in an ultra-stable clock application unless a hot filament was present. It is worth noting that even without a RGA or ion gauge, the trapped ion clocks have a hot electron emitter for generating an electron beam to load ions. This emitter, operated at a certain level, may be sufficient to crack methane.

Newer vacuum components, particularly optical window assemblies, now are rated to 450 C. With these installed on the L10 vacuum system, its bakeout temperature has been improved to greater than 400C. In addition, the bulk of the vacuum chamber is fabricated from titanium, which is known to have superior outgassing characteristics in UHV chambers. The resultant lower background gas evolution was observed in L10 in several ways. First, an integrated accumulation of several gases was monitored over a period of

several months by closing a valve separating the main clock vacuum tube from a residual gas analyzer (RGA). Upon opening the valve the pressure transient was observed (accounting for variations due simply to the valve itself). The transient placed a limit on methane gas evolution in the L10 vacuum chamber of about  $6 \times 10^{-16}$  torr/s or several orders of magnitude lower than that of the LITS-9 vacuum chamber.

The lifetime of  $\text{Hg}^+$  ions in the trap is largely governed by charge exchange with background gas molecules. Thus the trap lifetime is usually proportional to background gas pressure. With the new vacuum system, the L10 trap lifetime is now measured in days compared to tens of minutes for the older systems. Extrapolating from the known LITS-9 base pressure of about  $5 \times 10^{-10}$  torr, this indicates that the L10 pressure is less than  $1 \times 10^{-11}$  torr.

### *Magnetic Enhancements*

In addition to the magnetic design changes made in support of compensation, the C-field current source performance was enhanced. The evaluation in table 1 shows that magnetic sensitivity is one of the leading systematic effects in the clock. By updating components, the L10 current source has a temperature coefficient of 500 ppb, about an order of magnitude less sensitive to temperature variations than its predecessor in LITS-9. Current source aging has also been reduced.

### *Refractive optics – smaller more efficient*

LITS-9 used a reflective optics system with F/2 efficiency. It is possible to greatly reduce size and improve efficiency using refractive optics. The L10 design uses a custom asphere doublet for both input and output optics. The doublet is designed to minimize the point spread function so as to limit scattering off of nearby surfaces, while imaging the diffuse mercury plasma discharge 194 nm optical source onto the ion cloud and has a collection efficiency of F/1.2.

### *Low power DC electronics and Dedicated FPGA-based controller*

To improve reliability, reduce power consumption, and to reduce size, most commercial electronics used in LITS-9 were replaced by DC powered electronics. In addition, the obsolete VXI controller was replaced by a LINUX-based system running on an FPGA platform. Figures 2 and 3 show L10 configured with its DC-powered electronics modules in place and the FPGA-based controller respectively.

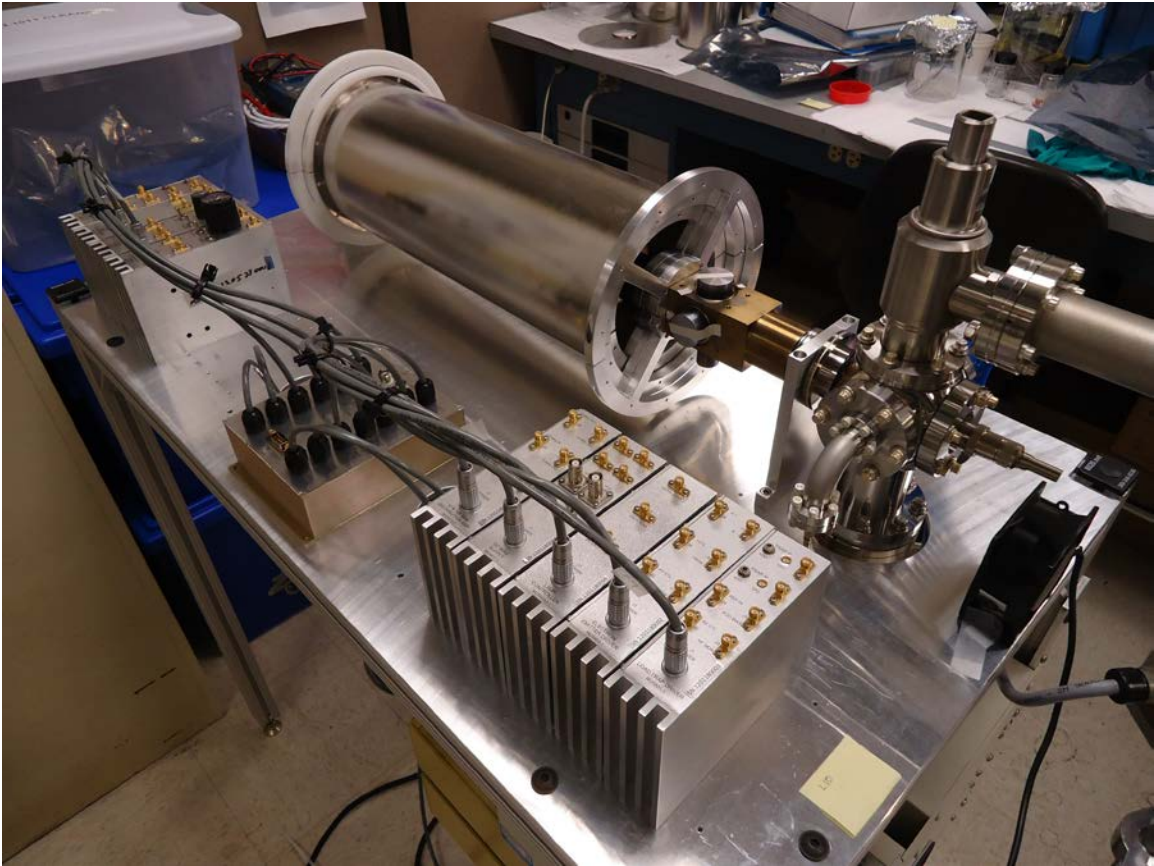


*Figure 2. L10 configured with DC-powered electronics. The physics package in the background has one magnetic shield layer installed.*



*Figure 3. FPGA-based L10 controller.*

### *Reduced size*

With an eye towards possible industrialization and further hardening, the overall size of the L10 system has been significantly reduced from LITS-9. Figure 4 shows a CAD cutaway of the L10 physics package. For scale, the stand that it is mounted on is about 36 inches long by 18 inches wide. There is still a large amount of potential for further reduction in size, and the key component dimensions are already consistent with the dimension of a standard rack mount chassis.

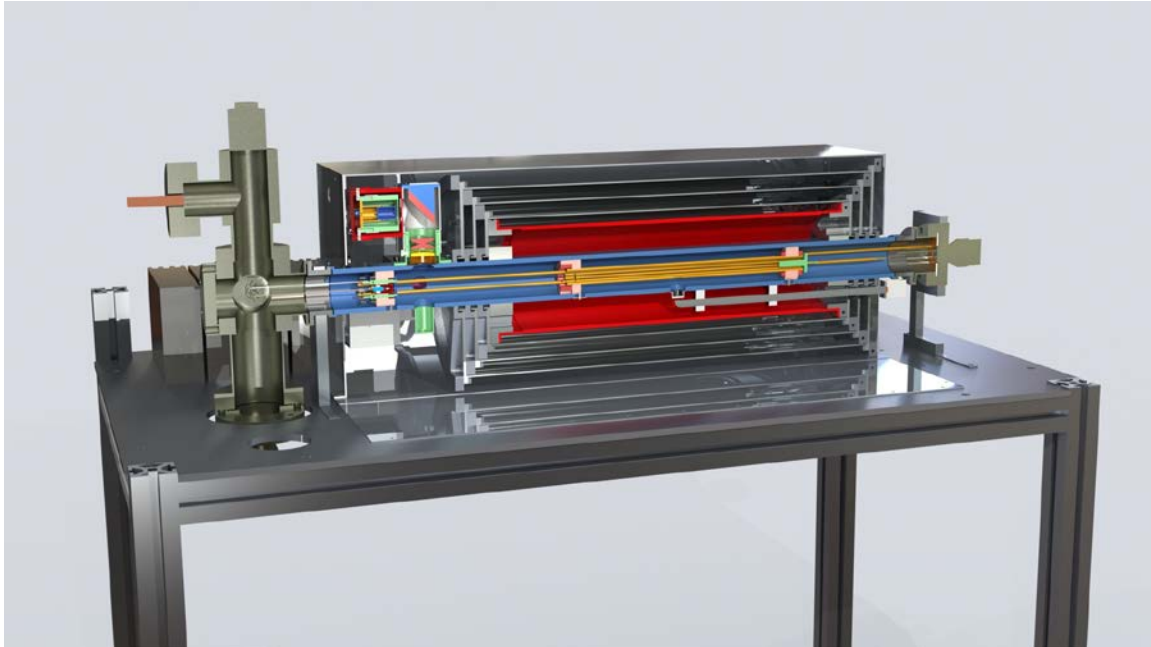


*Figure 4. A CAD cutaway view of the L10 physics package. The nested gray cylinders are magnetic shielding. These surround the solenoid shown in red, the vacuum chamber shown in blue and the multi-pole trap region shown in yellow.*

### **Initial Data**

After a design and fabrication phase in 2011-2012, L10 became operational in late 2012. In 2013 all subsystems of L10 were individually checked out and system level testing started. Here we give an overview of the results obtained to date.

### *Shuttling Efficiency*

“Shuttling” is the process of electro-magnetically moving ions from the quadrupole trap, in which they are loaded, to the multi-pole trap where sensitive clock microwave interrogation takes place. This process has two key benefits: 1) during critical clock operation, the ions are well away from perturbing effects such as residual un-blocked light from the light source, and 2) it places the ions in the multi-pole trap, making the clock largely immune to changes in ion number. It is easier to load and state prepare ions

in the quadrupole trap and shuttling allows the unique benefits of both traps to be used in the same clock. It is essential and not trivial to move 100% of the ions back and forth between the two traps. Figure 5 shows ions being shuttled between the quadrupole trap and the multi-pole trap many times, demonstrating 100% efficiency on a single transfer and near 100% efficiency even after 10 transfers of the same group of ions.

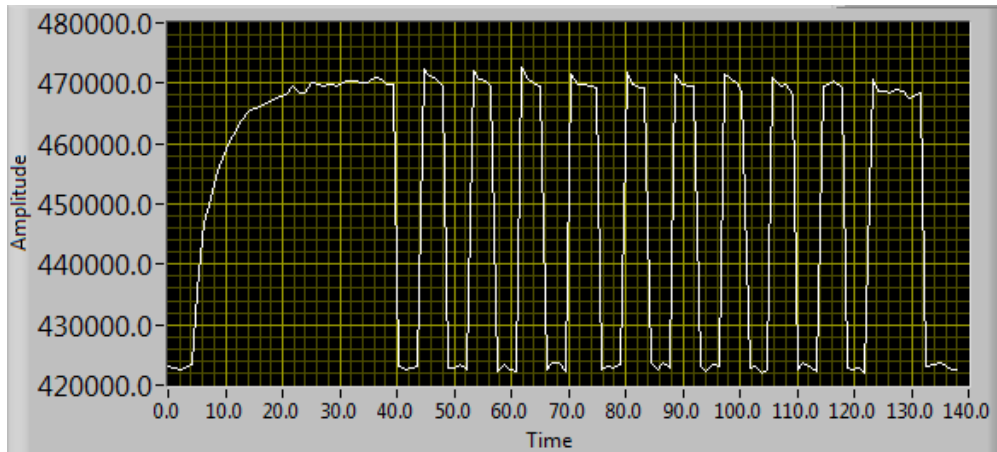


*Figure 5. A screen shot showing multiple shuttling of the same group of ions between the quadrupole and multi-pole traps and excellent control of the shuttling process. The graph shows fluorescence vs. time. Initially the ions are loaded into the quadrupole trap (where the detection region is) with an exponential time constant. As ions are moved out of the quadrupole trap, the fluorescence disappears. When the ions are moved back, 100% of the fluorescence reappears indicating a complete transfer of ions.*

### *Clock Performance*

The L10 physics package was initially configured with a hydrogen maser LO since this is how it will be operated at NRL. It could just as well be configured with a crystal LO for stand-alone operation. Using a maser LO, figure 6 shows a scan of the microwave interrogation frequency across the  $F=0, m=0 - F'=1, m'=0$  clock transition. This particular scan used Rabi interrogation with a 1 second Rabi time resulting in a 0.8 Hz FWHM.

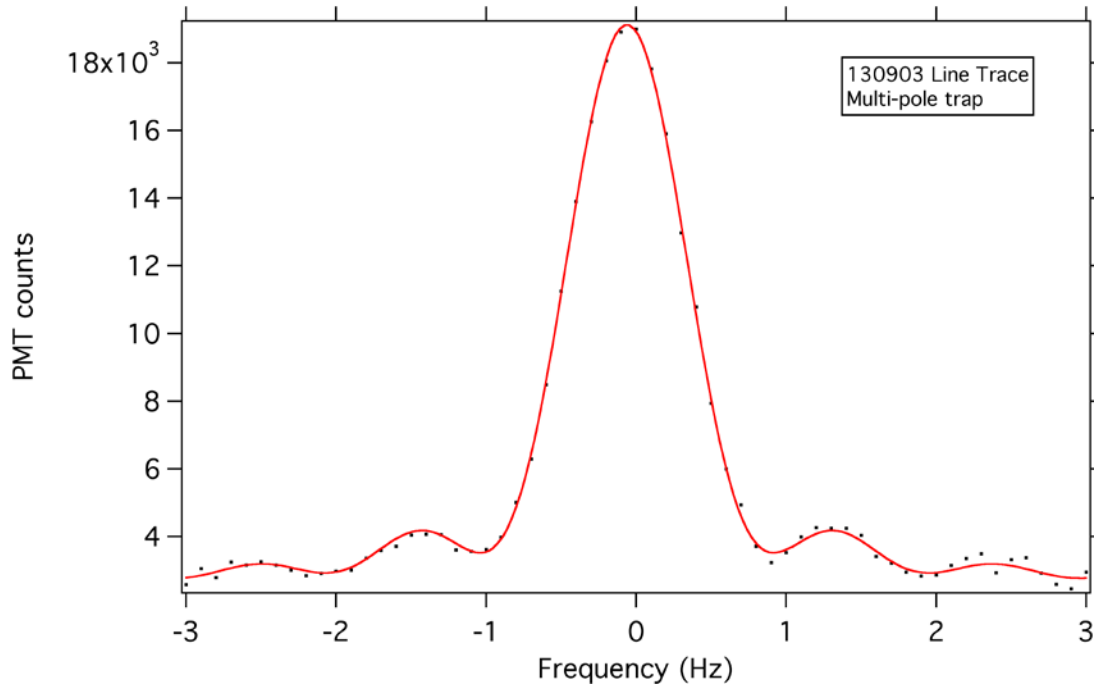


*Figure 6. Microwave frequency scan across the Hg+ clock transition.*

Figure 7 shows the short term Allan Deviation of frequency differences between L10 and the maser LO. Here the clock is operating with a 2 second Rabi interrogation time. Data past 1 day of averaging is not shown because it is simply dominated by maser drift. This Allan Deviation shows a modest short-term stability of about  $4.5 \times 10^{-13} / \tau^{1/2}$ . Better short-term stability will be achieved by increasing the interrogation time from the current 2 s to 10-20 s and by the addition of a second detection arm.

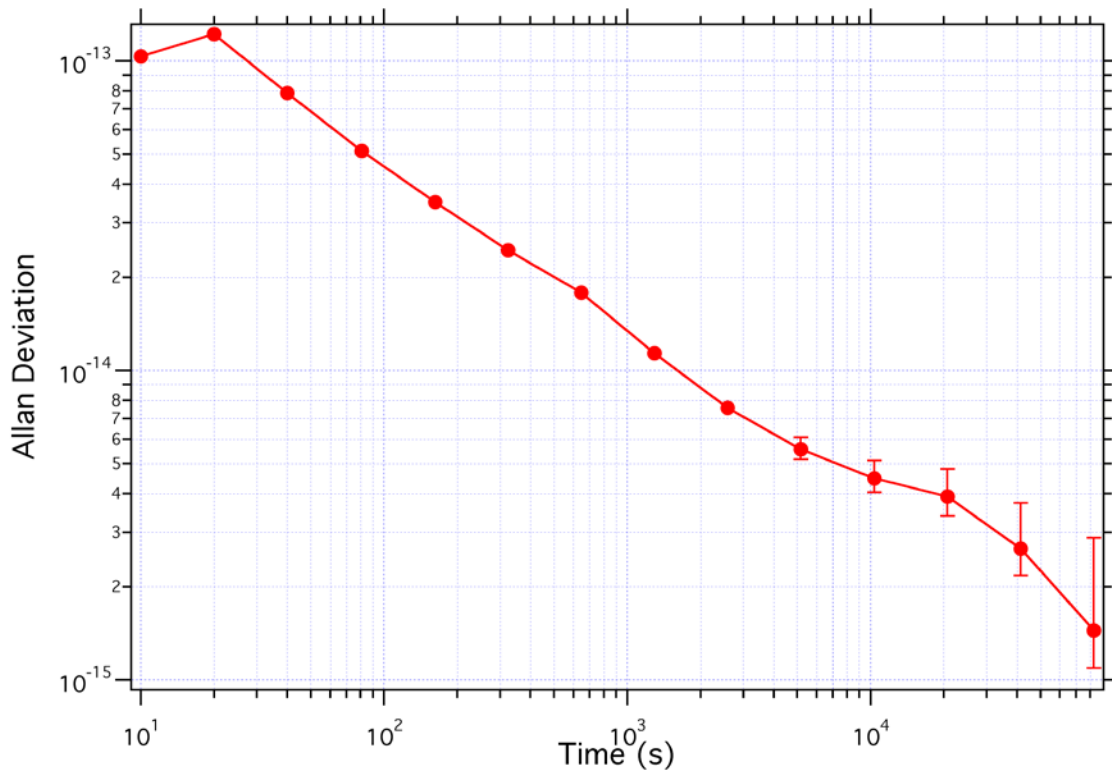


Figure 7. Allan Deviation of fractional frequency differences between L10 and its maser LO using a 2 second Rabi time and 1 detection arm.

At present, we do not yet have long-term stability data for L10; only comparisons to a maser, which is dominated by maser drift after about 1 day of averaging time. However, the unit has been moved into the JPL frequency standards test lab where it is steering the output of a maser. This output will be used to reference a GPS timing receiver for the month of December 2013, enabling comparison, via GPS, to UTC over that 30-day period. After this, final packaging will be installed and the unit shipped to NRL.

## Conclusion

In this paper we have described the development of a new compensated multi-pole trapped ion atomic clock, L10, for future reference use at the NRL. This new clock has several design improvements over its predecessor, LITS-9, most notably, engineered compensation of relativistic ion number dependent effects, improved vacuum, improved magnetic design, increased optical efficiency, and reduced mass, power, and volume. L10 is operating and is in the process of long-term evaluation. An identical copy of this clock has been built and will operate at JPL. Parts for a third unit are being ordered. The expected long-term stability of these units will be useful in characterizing other atomic clocks at NRL as well as in characterizing masers for use in NASA's Deep Space Network. In the 2016 time frame one of these units will also serve as an ultra-stable reference for the ACES microwave link ground terminal installed at JPL [14].

## Acknowledgements

The authors would like to thank D. Enzer for her careful characterization of the microwave coupling scheme used in L10, and J. Prestage for modeling of the multi-pole trap potential.

## References

- [1] D. Matsakis, P. Koppang, and R.M. Garvey, Proceedings of the 36<sup>th</sup> PTTI (2004).
- [2] R.L. Tjoelker, J.D. Prestage, P.A. Koppang, T.B. Swanson, "Stability Measurements of a JPL Multi-pole Mercury Trapped Ion Frequency Standard at the USNO," proceedings of the 2003 Joint Meeting of the 17<sup>th</sup> EFTF and 58<sup>th</sup> Ann. Symp. On Frequency Control, Tampa, FL; May 5-8, 2003.
- [3] E.A. Burt, W.A. Diener and R.L. Tjoelker, IEEE TUFFC **55**, 2586 (2008).
- [4] R.L. Tjoelker, C. Bricker, W. Diener, R.L. Hamell, A. Kirk, P. Kuhnle, L. Maleki, J.D. Prestage, D. Santiago, D. Seidel, D.A. Stowers, R.L. Sydnor, T. Tucker, "A Mercury Ion Frequency Standard Engineering Prototype for the NASA Deep Space Network," proceedings of the 50<sup>th</sup> Annual IEEE IFCS, Honolulu, Hawaii June 5-7, 1996.
- [5] J.D. Prestage, R.L. Tjoelker, and L. Maleki, "Higher Pole Linear Traps for Atomic Clock Applications," proceedings of the 1999 Joint Meeting EFTF - IEEE IFCS.
- [6] E.A. Burt, D. G. Enzer, R.T. Wang, W.A. Diener, and R.L. Tjoelker, proceedings of the 2006 PTTI, Reston, VA (2006).
- [7] G. Petit, "Atomic time scales TAI and TT(BIPM): present performances and prospects," Highlights of Astronomy **15**, 220 (2010).
- [8] E.A. Burt, S. Taghavi, J.D. Prestage, and R.L. Tjoelker, Proceedings of the 2008 IFCS, Hawaii (2008).
- [9] T.M. Fortier, et al., Nature Photonics **5**, 425 (2011).
- [10] R.L. Tjoelker, E.A. Burt, S. Chung, R.L. Hamell, J.D. Prestage, B. Tucker, P. Cash, and R. Lutwak, "Mercury atomic frequency standards for space based navigation and timekeeping," proceedings of the 43<sup>rd</sup> annual PTTI (2011).
- [11] J.D. Prestage, S. Chung, L. Lim, and T. Le, Proceedings of the 38<sup>th</sup> PTTI (2006); LITS-9 was also modified to operate with a sealed vacuum pumped by a getter and ran that way for a year. Its stability during that period was comparable to that of its mechanically pumped version.

[12] S.K. Chung, J.D. Prestage, and R.L. Tjoelker, Proceedings of the 2004 IEEE IFCS (2004); L. Yi, S. Taghavi-Larigani, E.A. Burt, and R.L. Tjoelker, Proceedings of the 2012 IEEE IFCS (2012).

[13] G.L. Shen, "The pumping of methane by an ionization assisted Zr/Al getter pump," J. Vac. Sci. Technol. **A 5**, 2580 (1987)

[14] L. Cacciapuoti and C. Salomon, Journal of Physics: Conference Series **327**, 012049 (2011)